

# Dark Matter and Dark Energy from a single scalar field

Roberto Mainini, Loris Colombo, Silvio A. Bonometto

Dipartimento di Fisica G. Occhialini, Università di Milano-Bicocca, Piazza della Scienza 3, 20126 Milano, Italy & I.N.F.N., Sezione di Milano

The strong CP problem was solved by Peccei & Quinn by introducing axions, which are a viable candidate for DM. Here the PQ approach is modified so to yield also Dark Energy (DE), which arises in fair proportions, without tuning any extra parameter. DM and DE arise from a single scalar field and, in the present epoch, are weakly coupled. Fluctuations have a fair evolution. The model is also fitted to WMAP release, using a MCMC technique, and performs as well as LCDM, coupled or uncoupled Dynamical DE. Best-fit cosmological parameters for different models are mostly within 2- $\sigma$  level. The main peculiarity of the model is to favor high values of the Hubble parameter.

## 1. Introduction

Axions are likely to be the Dark Matter (DM) that cosmological data require. Axions arise from the solution of the strong  $CP$  problem proposed by Peccei & Quinn in 1977 ([1], PQ hereafter), who suggested that  $\theta$  parameter, in the effective lagrangian term

$$\mathcal{L}_\theta = \frac{\alpha_s}{2\pi} \theta G \cdot \tilde{G} \quad (1)$$

( $\alpha_s$ : strong coupling constant,  $G$ : gluon field tensor), causing  $CP$  violations in strong interactions, is a dynamical variable. Under suitable conditions  $\theta$  approaches zero in our epoch, so that the term (1) is suppressed, while residual  $\theta$  oscillations yield DM [2, 3].

In the PQ scheme,  $\theta$  is the phase of a complex field  $\Phi = \phi e^{i\theta}/\sqrt{2}$ ; its evolution is set by the potential

$$V(|\Phi|) = \lambda [|\Phi|^2 - F_{PQ}^2]^2, \quad (2)$$

whose  $U(1)$  invariance breaks when  $T < F_{PQ}$  (the PQ energy scale, which shall be  $\sim 10^{12}$  GeV). Then  $\phi$  settles at the potential minimum, while  $\theta$  takes a random value, different in different horizons. When chiral symmetry also breaks down, during the quark-hadron transition, a further term

$$V_1 = \left[ \sum_q \langle 0(T) | \bar{q}q | 0(T) \rangle m_q \right] (1 - \cos \theta) \quad (3)$$

must be added to the lagrangian, because of instanton effects. At  $T \simeq 0$ , the square bracket approaches  $m_\pi^2 f_\pi^2$  ( $m_\pi$ ,  $f_\pi$ :  $\pi$ -meson mass, decay constant).

The dependence on the site of initial  $\theta$ 's will causes later adjustments, as soon as the potential (3) switches on. When  $\theta$  is small,  $V_1 \propto \theta^2$  and the  $\theta$  field, undergoing harmonic oscillations, is DM.

Here we wish to discuss recent work [4], where the NG potential (2) is replaced by a tracker potential [5]. Then, instead of settling on a value  $F_{PQ}$ ,  $\phi$  continues to evolve over cosmological times, at any  $T$ . As in the PQ case, the potential involves a complex field  $\Phi$  and is  $U(1)$  invariant. Its phase is horizon-dependent

but, just as in the PQ case, evolves only after chiral symmetry breaks, yielding a term similar to (3).

At variance from the PQ case, however, the  $\theta$  evolution starts and continues while also  $\phi$  is still evolving. This goes on until our epoch, when  $\phi$  is expected to account for Dark Energy (DE), while, superimposed to such slow evolution, faster *transversal*  $\theta$  oscillations occur, accounting for DM. This scheme, where the  $\Phi$  fields bears a dual role, with its modulus and phase, will be dubbed here *dual axion model*.

The question is whether  $\phi$  and  $\theta$  dynamics interfere, still allowing  $\theta$  to take values so small to solve the  $CP$  problem and preserving harmonic oscillations allowing the prescribed amount of DM. Here we show that the reply is positive. As it can be expected, however, DM and DE are dynamically coupled, although this coupling weakens as we approach the present era.

Here we also consider a generalization of the SUGRA potential [5] as an example of tracker potential. With an energy scale  $\Lambda \sim 10^{10}$  GeV, this model allows suitable values for today's DM and DE densities, while  $\theta$  is even smaller than for PQ. DM density fluctuations are also able to grow and to account for the observed large scale structure. We fit the expected angular CBR spectra to data, finding that this model substantially performs as well as  $\Lambda$ CDM.

## 2. Lagrangian theory

In the dual-axion model we start from the lagrangian  $\mathcal{L} = \sqrt{-g} \{ g_{\mu\nu} \partial_\mu \Phi \partial_\nu \Phi - V(|\Phi|) \}$  which can be rewritten in terms of  $\phi$  and  $\theta$ , adding also the term breaking the  $U(1)$  symmetry, as follows:

$$\mathcal{L} = \sqrt{-g} \left\{ (1/2) g_{\mu\nu} [ \partial_\mu \phi \partial_\nu \phi + \phi^2 \partial_\mu \theta \partial_\nu \theta ] - V(\phi) - m^2(T, \phi) \phi^2 (1 - \cos \theta) \right\}.$$

Here  $g_{\mu\nu}$  is the metric tensor. We shall assume that  $ds^2 = g_{\mu\nu} dx^\mu dx^\nu = a^2 (d\tau^2 - \eta_{ij} dx_i dx_j)$ , so that  $a$  is the scale factor,  $\tau$  is the conformal time; greek (latin) indices run from 0 to 3 (1 to 3); dots indicate differentiation in respect to  $\tau$ . The mass behavior for

$T \sim \Lambda_{QCD}$  will be detailed in Section 3. The equations of motion read

$$\ddot{\theta} + 2(\dot{a}/a + \dot{\phi}/\phi) \dot{\theta} + m^2 a^2 \sin \theta = 0, \quad (4)$$

$$\ddot{\phi} + 2(\dot{a}/a) \dot{\phi} + a^2 V'(\phi) = \phi \dot{\theta}^2, \quad (5)$$

while the energy densities  $\rho_{\theta,\phi} = \rho_{\theta,\phi;kin} + \rho_{\theta,\phi;pot}$  and pressures  $p_{\theta,\phi} = \rho_{\theta,\phi;kin} - \rho_{\theta,\phi;pot}$ , under the condition  $\theta \ll 1$ , are obtainable from

$$\begin{aligned} \rho_{\theta,kin} &= \dot{\theta}^2/2a^2, & \rho_{\theta,pot} &= m^2(T,\phi)\phi^2\theta^2/2, \\ \rho_{\phi,kin} &= \dot{\phi}^2/2a^2, & \rho_{\phi,pot} &= V(\phi). \end{aligned} \quad (6)$$

### 3. Axion mass

According to eq. (4), the axion field begins to oscillate when  $m(T,\phi)a \simeq 2(\dot{a}/a + \dot{\phi}/\phi)$ . In the dual-axion model, just as for PQ, axions become massive when the chiral symmetry is broken by the formation of the  $\bar{q}q$  condensate at  $T \sim \Lambda_{QCD}$ . Around such  $T$ , therefore, the axion mass grows rapidly. In the dual-axion model, however, a slower growth takes place also later, because of the evolution of  $\phi$ . Then  $m(T,\phi)$  is

$$m_o(\phi) = m_\pi f_\pi / \phi = (0.0062/\phi) \text{ GeV}. \quad (7)$$

Since  $\phi \sim m_p$  today, the axion mass is now  $m_o \sim 5 \cdot 10^{-13} \text{ eV}$ , while, according to [6], at high  $T$ :

$$m(T,\phi) \simeq 0.1 m_o(\phi) (\Lambda_{QCD}/T)^{3.8}. \quad (8)$$

This expression must be interpolated with eq. (7), to study the fluctuation onset for  $T \sim \Lambda_{QCD}$ . We solved the equations of section 2 by assuming

$$\begin{aligned} m(T,\phi) &= m_o(\phi) (0.1)^{\frac{1}{3.8}} \Lambda_{QCD}/T)^{3.8(1-\frac{a}{a_c})} & a < a_c \\ m(T,\phi) &= m_o(\phi) & a > a_c \end{aligned}$$

with  $a_c = 2.16 \cdot 10^{-12}$ . With the selected value, when  $T \lesssim 0.5 \Lambda_{QCD}$ ,  $m(T,\phi)$  already approaches its low- $T$  behavior  $m_o(\phi)$ . Let us finally outline that eqs. (7) and (8), as well as the above interpolation, show that  $m(T,\phi)\phi$  is  $\phi$ -independent, as is required to obtain the equation of motion (5). Fig.(1) shows the (low-) $z$  dependence of  $m_o(\phi)$ . Notice the rebound at  $z \sim 10$ , whose impact on halo formation could be critical [7].

### 4. The case of SUGRA potential

When  $\theta$  performs many oscillations within a Hubble time, then  $\langle \rho_{\theta,kin} \rangle \simeq \langle \rho_{\theta,pot} \rangle$  and  $\langle p_\theta \rangle \simeq 0$ . By using eqs. (4),(5),(6), it is easy to see that

$$\dot{\rho}_\theta + 3H\rho_\theta = \frac{\dot{m}}{m} \rho_\theta, \quad \dot{\rho}_\phi + 3H(\rho_\phi + p_\phi) = -\frac{\dot{m}}{m} \rho_\theta. \quad (9)$$

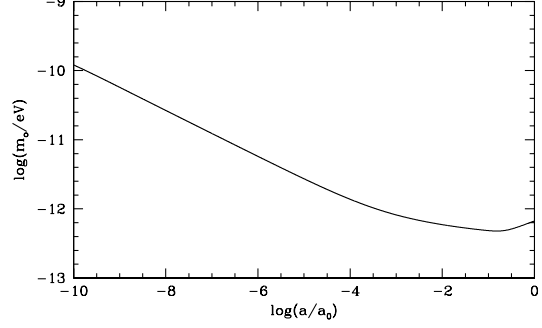


Figure 1:  $\phi$  variations cause a dependence of the effective axion mass on scale factor  $a$ , which is shown here.

When  $m$  is given by Eq (8),  $\dot{m}/m = -\dot{\phi}/\phi - 3.8\dot{T}/T$ . At  $T \simeq 0$ , instead,  $\dot{m}/m \simeq -\dot{\phi}/\phi$ . Here below, the indices  $\theta, \phi$  will be replaced by  $DM, DE$ . Eqs. (9) show an energy exchange between DM and DE. The former eq. (9) can then be integrated, yielding  $\rho_{DM} \propto m/a^3$ . This law holds also when  $T \ll \Lambda_{QCD}$ , and then the usual behavior  $\rho_{DM} \propto a^{-3}$  is modified, becoming

$$\rho_{DM} a^3 \phi \simeq \text{const}. \quad (10)$$

Let us now assume that the potential reads

$$V(\phi) = (\Lambda^{\alpha+4}/\phi^\alpha) \exp(4\pi\phi^2/m_p^2) \quad (11)$$

(no  $\theta$  dependence); in the radiative era, it will then be

$$\phi^{\alpha+2} = g_\alpha \Lambda^{\alpha+4} a^2 \tau^2, \quad (12)$$

with  $g_\alpha = \alpha(\alpha+2)^2/4(\alpha+6)$ . This tracker solution holds until we approach the quark-hadron transition. Then, in Eq. (5), the DE-DM coupling term,  $\phi\dot{\theta}^2$ , exceeds  $a^2 V'$  and we enter a different tracking regime.

This is shown in detail in Fig.(2), obtained for matter (baryon) density parameters  $\Omega_m = 0.3$  ( $\Omega_b = 0.03$ ) and Hubble constant  $h = 0.7$  (in units of 100 km/s/Mpc). In particular, Fig. (2a) shows the transition between these tracking regimes. Fig. (2b) then shows the low- $z$  behavior ( $1+z = 1/a$ ), since DE density exceeds radiation ( $z \simeq 100$ ) and then overcomes baryons ( $z \simeq 10$ ) and DM ( $z \simeq 3$ ). Fig. (2c) is a landscape picture for all components, down to  $a = 1$ .

Notice the  $a$  dependence of  $\rho_{DM}$ , occurring according to Eq. (10). In Fig. (3) the related behaviors of the density parameters  $\Omega_i$  ( $i = r, b, \theta, \phi$ , i.e. radiation, baryons, DM, DE) are shown.

In general, once the density parameter  $\Omega_{DE}$  (at  $z = 0$ ) is assigned, a model with dynamical (coupled or uncoupled) DE is not yet univocally determined. For instance, the potential (11) depends on the parameters  $\alpha$  and  $\Lambda$  and one of them can still be arbitrarily fixed. Other potentials show similar features.

In this model such arbitrariness no longer exists. Let us follow the behavior of  $\rho_{DM}$ , backwards in time,

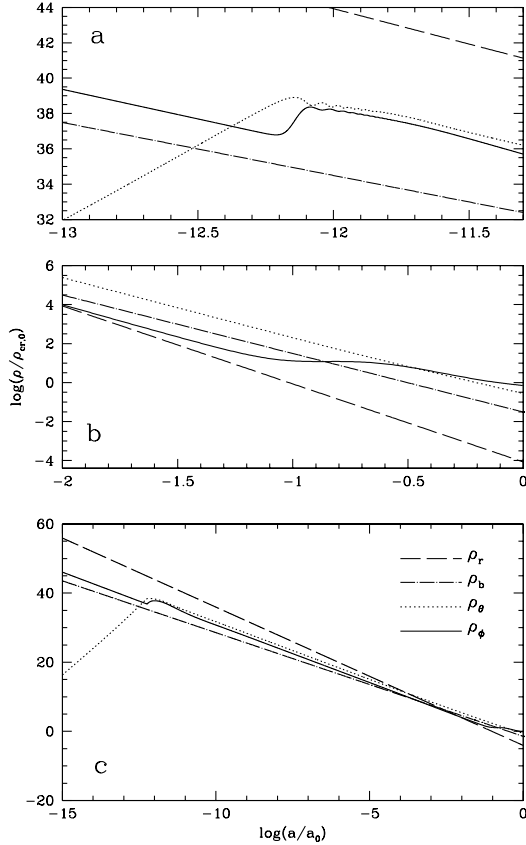


Figure 2: Density behaviors vs. scale factor.

until the approximation  $\theta \ll 1$  no longer applies. This must approximately coincide with the time when

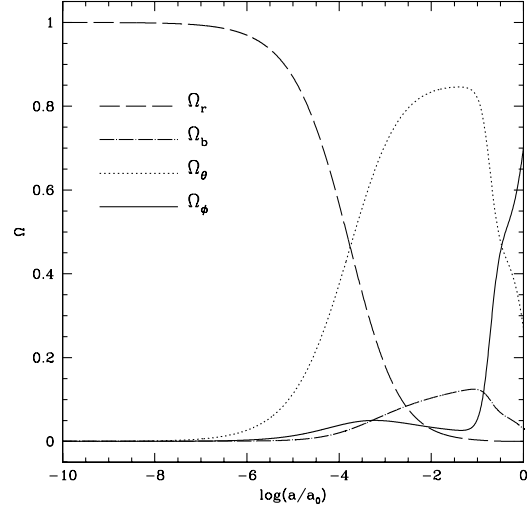
$$2(\dot{a}/a + \dot{\phi}/\phi) \simeq m(T, \phi) a \quad (13)$$

and  $\theta$  enters the oscillation regime. At that time, according to Eq. (10), which is marginally valid up to there, and taking  $\theta = 1$ ,

$$\rho_{DM} \simeq \rho_{o,DM} \frac{\phi_o}{\phi(a)} \frac{1}{a^3} \simeq m^2 [T(a), \phi(a)] \phi^2(a). \quad (14)$$

The system made by eqs. (13) and (14), owing to eq. (12), allows to obtain (i) the scale factor  $a_h$  when fluctuations start and (ii) the scale  $\Lambda$  in the potential (11). To do so, the present density of DM,  $\rho_{o,DM}$ , (or  $\Omega_{DM}$ ) must be assigned. But, as we shall soon outline, the observational value of the density in the world forces  $a_h$  to lay about the quark–hadron transition, while also  $\Lambda$  is substantially fixed.

The plots in the previous section are for  $\Omega_{DM} = 0.27$ ; then  $\Lambda \simeq 1.5 \cdot 10^{10} \text{GeV}$  and  $a_h \sim 10^{-13}$  are required by the system. But, when  $\Omega_{DM}$  goes from 0.2 to 0.4,  $\log_{10}(\Lambda/\text{GeV})$  (almost) linearly runs in the narrow interval 10.05–10.39, while  $a_h$  steadily lays at the eve of the quark–hadron transition.


 Figure 3: Density parameters  $\Omega_i$  vs. scale factor  $a$ .

## 5. Evolution of inhomogeneities

Besides of predicting fair ratios between the world components, a viable model should also allow the formation of structures in the world.

The dual axion model belongs to the class of coupled DE models treated by Amendola [8], with a time–dependent coupling  $C(\phi) = 1/\phi$ . A  $\phi$ – $MDE$  phase therefore exists, after matter–radiation equivalence, as the kinetic energy of DE is non–negligible during the matter–dominated era.

Fluctuation evolution is then obtained by solving the equations in [7], with the above  $C(\phi)$ . The behavior shown in Fig.(4) (left) is then found.

Fig (4) (center and right) compare fluctuation evolutions the dual axion model (solid curves), with those in an analogous  $\Lambda$ CDM model (dot–dashed curves) and in a coupled DE model with constant coupling  $C = 0.25 \sqrt{8\pi G} \simeq \langle C(\phi) \rangle$  (dashed curves). As shown by the plots, the overall growth, from recombination to now is similar in dual axion and  $\Lambda$ CDM models, being quite smaller than in DE models with constant coupling. The differences of dual axion from  $\Lambda$ CDM are: (i) objects form earlier and (ii) baryon fluctuations keep below DM fluctuations until very recently.

## 6. Comparison with WMAP data

We shall then test the dual axion model towards CMB data, together with other dynamical or coupled DE cosmologies, by using a parameter space of 7 to 8 dimensions. We use a Markov Chain Monte Carlo (MCMC) approach (e.g. [9]), just as in the original analysis of WMAP first–year data [10], constraining

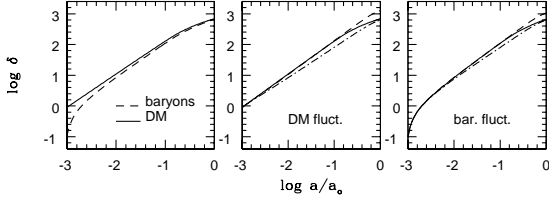


Figure 4: Time evolution of DM and baryon fluctuations.

flat  $\Lambda$ CDM in respect to six parameters:  $\Omega_b h^2$ ,  $\Omega_m h^2$ ,  $h$ ,  $n$ , the fluctuation amplitude  $A$  and the optical depth  $\tau$ . Notice that, with the naming convention used here,  $\Omega_m \equiv \Omega_b + \Omega_{DM}$ .

Here, three classes of DE are considered: (i) SUGRA dynamical DE, requiring the introduction of the parameter  $\lambda = \log_{10}(\Lambda/\text{GeV})$ , the energy scale in the potential (12). (ii) Constant coupling SUGRA DE, requiring a further parameter, the coupling  $\beta = C(3m_p^2/16\pi)^{1/2}$ . (iii) Coupled models including the dual axion case. For this model the parameter  $\beta$  does not exist, being  $C = \phi^{-1}$  and also the scale  $\Lambda$  is constrained by the requirement that  $\Omega_{DE}$  lays in a fair range (also solving the strong  $CP$  problem), so that  $\Lambda$  and  $\Omega_{DE}$  are no longer independent parameters. The (iii) class of model, that we call  $\phi^{-1}$  models, is however set keeping  $\lambda$  as a free parameter. We aim to test whether data constrain  $\lambda$  into the right region, turning a generic  $\phi^{-1}$  model into a dual-axion model.

To use the MCMC, we need an algorithm providing the  $C_l$ 's. Here we use our optimized extension of CMBFAST [11], able to inspect the cosmologies (i), (ii) and (iii). Then, the likelihood of each model is evaluated through the publicly available code by the WMAP team [12] and accompanying data [13].

## 6.1. Results

The basic results of our analysis are summarized in the Table I, II and III. For each model category we list the expectation values  $\langle x \rangle$  of each parameter  $x$  and the associated variance  $\sigma_x$ ; we also list the values of the parameters of the best fitting models  $x_{max}$ .

Let us however remind that  $\phi^{-1}$  models, whose fitting results are reported in Table III, include the dual-axion model, but many other cases as well. Our approach was meant to test whether CMB data carry information on  $\lambda$  and how this information fits the  $\lambda$  range turning a  $\phi^{-1}$  model into the dual-axion model.

At variance from uncoupled and constant-coupling SUGRA models, WMAP data yield constraints on  $\lambda$  for  $\phi^{-1}$  models (see Table III) and the  $2\text{-}\sigma$   $\Lambda$ -interval ranges from  $\sim 10$  to  $\sim 3 \cdot 10^{10}$  GeV, so including the dual-axion model. In Fig. (5) the  $C_l^T$  spectra for all best-fit models (apart of  $\Lambda$ CDM) are compared. At

Table I SUGRA parameters for uncoupled DE

$x$	$\langle x \rangle$	$\sigma_x$	$x_{max}$
$\Omega_b h^2$	0.025	0.001	0.026
$\Omega_{DM} h^2$	0.12	0.02	0.11
$h$	0.63	0.06	0.58
$\tau$	0.21	0.07	0.28
$n_s$	1.04	0.04	1.08
$A$	0.97	0.13	1.11
$\lambda$	3.0	7.7	13.7

Table II SUGRA parameters in the presence of a constant DE-DM coupling  $\beta$ .

$x$	$\langle x \rangle$	$\sigma_x$	$x_{max}$
$\Omega_b h^2$	0.024	0.001	0.024
$\Omega_{DM} h^2$	0.11	0.02	0.12
$h$	0.74	0.11	0.57
$\tau$	0.18	0.07	0.17
$n_s$	1.03	0.04	1.02
$A$	0.92	0.14	0.93
$\lambda$	-0.5	7.6	8.3
$\beta$	0.10	0.07	0.07

Table III SUGRA parameters for a  $\phi^{-1}$  model.

$x$	$\langle x \rangle$	$\sigma_x$	$x_{max}$
$\Omega_b h^2$	0.025	0.001	0.026
$\Omega_{DM} h^2$	0.11	0.02	0.09
$h$	0.93	0.05	0.98
$\tau$	0.26	0.04	0.29
$n_s$	1.23	0.04	1.23
$A$	1.17	0.10	1.20
$\lambda$	4.8	2.4	5.7

large  $l$  all models yield similar behaviors and this is why no model category prevails. Discrimination could be achieved by improving large angular scale observation, especially for polarization, so to reduce the errors on small- $l$  harmonics.

## 7. Discussion

A first point worth outlining is that SUGRA (uncoupled) models, bearing precise advantages in respect to  $\Lambda$ CDM, are consistent with WMAP data. The ratio  $w = p/\rho$  at  $z = 0$ , for most these models, fulfills the constraint  $w \lesssim -0.80$ . However, these models exhibit a fast  $w$  variation, and  $w$  becomes  $\sim$

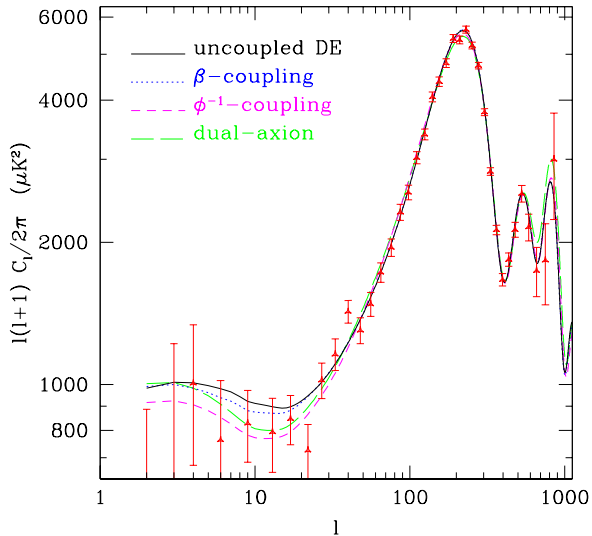


Figure 5:  $C_l^T$  spectra for the best fit SUGRA (solid line), constant coupling (dotted line),  $\phi^{-1}$ -coupling (dashed) and dual-axion (dot-dashed) models.

-0.6, -0.7 at  $z \sim 1-2$ . In spite of this sharp decrease, however, there is no conflict with data.

The results shown in the previous section were also considered in the presence of some priors. For uncoupled or constant-coupling SUGRA models, adding priors scarcely affects conclusions.  $\phi^{-1}$ -models, instead, are to be discussed separately.

In the first two categories of models opacity ( $\tau$ ) is pushed to values even greater than in  $\Lambda$ CDM (see also [14]). This can be understood in two complementary ways: (i) Dynamical DE models, in general, exhibit a stronger ISW effect, increasing  $C_l^T$  in the low- $l$  plateau (e.g. [15]). To compensate this effect, in the fit of data, the spectral index  $n_s$  is pushed to greater values. In turn, owing to the  $\tau$ - $n$  degeneracy, this is compensated by increasing  $\tau$ . (ii) If the TE correlation is also considered, it is worth reminding that dynamical DE lowers the TE correlation at low  $l$  [16]. To fit the same observed correlation level, a greater  $\tau$  is therefore favored.

Greater  $\tau$ 's have an indirect impact also on  $\Omega_b h^2$  whose best-fit value becomes greater, although consistent with  $\Lambda$ CDM within  $1-\sigma$ . If we impose, as a prior,  $\Omega_b h^2 = 0.0214 \pm 0.0020$  (BBNS estimates [17]),  $h$  shifts slightly below HST findings, still well within  $1-\sigma$ . We shall consider the effect of a prior also on  $h$ .

The prior on  $\Omega_b h^2$  affects reionization and the spectral slope:  $\tau$  and  $n_s$  are lowered to match WMAP's findings. The prior on  $h$ , in the absence of coupling, favors low- $\lambda$  models, closer to  $\Lambda$ CDM. Quite in general, in fact, the sound horizon at decoupling is unaffected by the energy scale  $\Lambda$ , while the distance of the last-scattering-band is smaller for greater  $\lambda$ 's. Then, as  $\lambda$  increases, a lower  $h$  is favored to match the position of the first peak. In the presence of coupling, there is a simultaneous effect on  $\beta$ : greater  $\beta$ 's yield

a smaller sound horizon at recombination, so that the distribution on  $h$  is smoother.

$\phi^{-1}$  models exhibit rather different features. Parameters are more strongly constrained in this case, as already outlined for the scale  $\Lambda$ . The main puzzling feature of  $\phi^{-1}$  models is that large  $h$  is favored: the best-fit  $2-\sigma$  interval does not extend below 0.85.

The problem is more severe for dual-axion  $\lambda$ 's values, whose preferred values are well within  $2-\sigma$ . This model naturally tends to displace the first  $C_l^T$  peak to greater  $l$  (smaller angular scales) as coupling does in any case does. The model, however, has no extra coupling parameter and the intensity of coupling is controlled by the scale  $\Lambda$ . Increasing this scale requires a more effective compensation and still greater values of  $h$  are favored.

This effect appears however related to the choice of SUGRA potentials, which is just meant to provide a concrete framework for the dual axion model. To deepen its analysis, the contribution to the axion abundance due to the decay of possible topological defects should also be discussed.

A previous analysis of WMAP limits on constant coupling models had been carried on by [19]. Their analysis concerned potentials  $V$  fulfilling the relation  $dV/d\phi = BV^N$ , with suitable  $B$  and  $N$ . They also assumed that  $\tau \equiv 0.17$ . Our analysis deals with a different potential and allows more general parameter variations. The constraints on  $\beta$  we find are less severe. It must be however outlined that  $\beta > 0.1-0.2$  is forbidden by a non-linear analysis of structure formation [7].

## 8. Conclusions

The first evidences of DM date some 70 years ago, although only in the late Seventies limits on CMB anisotropies made evident that a non-baryonic component had to be dominant. DE could also be dated back to Einstein's *cosmological constant*, although only SNIa data revived it, soon followed by data on CMB and deep galaxy samples.

Axions have been a good candidate for DM since the late Seventies, although various studies, as well as the occurrence of the SN 1987a, strongly constrained the PQ scale around values  $10^{10} \lesssim F_{PQ} \lesssim 10^{12} \text{GeV}$ . Contributions to DM from topological singularities (cosmic string and walls) narrowed the constraints to  $F_{PQ}$ . Full agreement on the relevance of such contributions has not yet been attained and, in this paper, they are still disregarded, while they could cause shifts in our quantitative predictions. This point must be therefore deepened in further work.

The fact that DM and DE can both arise from scalar fields, just by changing the power of the field in effective potentials, already stimulated the work of various authors. A potential like (11) was considered in the

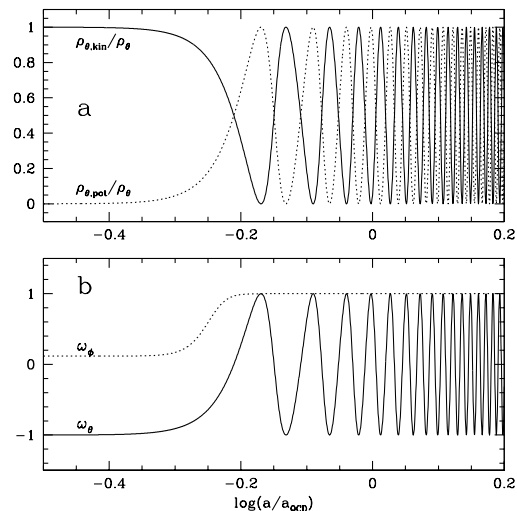


Figure 6: The onset of coherent axion oscillations, due to the increase of  $m(T, \phi)$ , causes the behaviors of  $\rho_{\theta,pot}$ ,  $\rho_{\theta,kin}$  (a) and  $\omega_{\phi,\theta} = p_{\phi,\theta}/\rho_{\phi,\theta}$  (b) shown here.

so-called *spintessence* model [20]. According to the choice of parameters,  $\Phi$  was shown to behave either as DM or as DE. Padmanabhan & Choudhury [21], instead, built a tachionic model where DM and DE arise from a single scalar field.

Here, the scalar field  $\Phi$ , accounting for *both* DE and DM, arises in the solution of the strong- $CP$  problem: as in the PQ model, in eq. (1)  $\theta$  is turned into a dynamical variable, the phase of  $\Phi$ . Here, however, the modulus of  $\Phi$  increases in time, approaching  $m_p$  by our cosmic epoch, when it is DE; meanwhile,  $\theta$  is driven to approach zero, still performing harmonic oscillations which are axion DM. The critical time for the onset of coherent axion oscillations is the eve of the quark-hadron transition, because of the rapid increase of the axion mass  $m(T, \phi)$ . In our dual axion scheme, the constant  $F_{PQ}$  scale of the PQ model is replaced by the slowly varying field  $\phi$ . Instead of the scale  $F_{PQ}$ , data fix the scale  $\Lambda$ , in the SUGRA potential. This unique setting provides DM and DE in fair proportions.

We therefore simultaneously solve the strong  $CP$  problem and yield DM and DE in fair proportions by setting a single parameter.

## References

- [1] Peccei R.D. & Quinn H.R. 1977, Phys.Rev.Lett. 38, 1440; but see also: Kim J.E. 1979, Phys.Rev.Lett. 43, 103.
- [2] Weinberg S. 1978, Phys.Rev.Lett. 40, 223; Wilczek F. 1978, Phys.Rev.Lett. 40, 279
- [3] Preskill J. et al 1983, Phys.Lett B120, 225; Abbott L. & Sikivie P. 1983 Phys.Lett B120, 133; Dine M. & Fischler 1983 Phys.Lett B120, 137; Turner M.S. 1986 Phys.Rev.D 33, 889.
- [4] Mainini R. & Bonometto S.A., 2004, Phys.Rev.Lett. 93, 121301; Mainini R., Colombo L.P.L., & Bonometto S.A, 2005, ApJ submitted, astro-ph/0503036
- [5] Wetterich C., 1995 A&A 301, 32; Ratra B. & Peebles P.J.E., 1988, Phys.Rev.D, 37, 3406; Ferreira G.P. & Joyce M. 1998 Phys.Rev.D 58, 023503; Brax, P. & Martin, J., 1999, Phys.Lett., B468, 40; Brax, P. & Martin, J., 2001, Phys.Rev. D, 61, 10350; Brax P., Martin J., Riazuelo A., 2000, Phys.Rev. D, 62, 103505
- [6] Kolb R.W. & Turner M.S. 1990 The Early Universe, Addison Wesley, and references therein
- [7] Macciò A., Quercellini C., Mainini R., Amendola L., Bonometto S.A. 2004 Phys.Rev.D (in press), astro-ph/0309671; see also Mainini R., Macciò A.V., Bonometto S.A., Klypin A. 2003 Ap.J. 599, 24; Klypin A., Macciò A.V., Mainini R., Bonometto S.A. 2003 Ap.J. 599, 31.
- [8] Amendola L. 2000, Phys.Rev D 62, 043511; Amendola L. 2003 Phys.Rev.D (subm.) and astro-ph/0311175
- [9] Christensen N., Meyer R., Knox L. & Luey, B. 2001, Classical and Quantum Gravity, 18, 2677; Knox L., Christensen, N. & Skordis C. 2001, ApJ 63, L95; Lewis, A. & Bridle, S. 2002, Phys.Rev. D 66, 103511; Kosowsky A., Milosavljevic M. & Jimenez R. 2002, Phys.Rev.D 66, 63007; Dunkley J., et al. 2004, MNRAS, submitted, astro-ph/0405462, 2004
- [10] Spergel D.N. et al., 2003, ApJ Suppl. 148, 175
- [11] Seljak U. & Zaldarriaga M. 1996, ApJ, 469 437
- [12] Verde et al. 2003, ApJ Suppl., 148, 195
- [13] Hinshaw G., et al. 2003, ApJ Suppl., 148, 135; Kogut A., et al. 2003, ApJ Suppl., 148, 161
- [14] Corasaniti P.S., et al. 2004, Phys. Rev. D, in press, astro-ph/0406608
- [15] Weller J. & Lewis A.M. 2003, MNRAS, 346, 987
- [16] Colombo L.P.L., Mainini R. & Bonometto S.A. 2003, in proceedings of Marseille 2003 Meeting, 'When Cosmology and Fundamental Physics meet'
- [17] Kirkman D. et al. 2003, ApJS, 149, 1
- [18] Ciardi B., Ferrara A. & White S.D.M. 2003, MNRAS, 344, L7; Ricotti M. & Ostriker J.P. 2004, MNRAS, 350, 359
- [19] Amendola L. & Quercellini C. 2003, Phys. Rev. D69, 023514
- [20] Boyle L.A., Caldwell R.R. & Kamionkowski M. 2002, Phys. Lett. B545, 17; Gu Je-An & Hwang W-Y. P. 2001, Phys. Lett. B517, 1
- [21] Padmanabhan T., Choudhury T.R., 2002, Phys.Rev. D66, 081301.